Relais Request No. REG-30233985

Customer Code	Delivery Method	Request Number
34-0076	**SED**	**RZUTP 098 SED99 COPYRT S**

Scan

Date Printed: 17-Feb-2012 07:24
Date Submitted: 14-Feb-2012 02:42

3839.355000
TITLE: EXPERIMENTAL HEAT TRANSFER, FLUID
YEAR: 1988
VOLUME/PART:
PAGES:
AUTHOR:
ARTICLE TITLE:
SHELFMARK: 3839.355000

INFORMATION RESOURCE CENTRE

Your Ref :
RZUTP 098 SED99 COPYRT S S|EXPERIMENTAL HEAT TRANSFER, FLUID|MECHANICS AND THERMODYNAMICS 1988 :|SHAH, R. K. (RAMESH K.)|1988.|A FLYING HOT-WIRE PROBE SYSTE|BRUUN, H.H., JAJU, A.A., AL-KAYIEM, H.H.|ELSEVIER, NEW YORK

A FLYING HOT-WIRE PROBE SYSTEM FOR MEASUREMENTS IN SEPARATED FLOW

H H Bruun, A A R Jaju, H H Al-Kayiem and M A Khan

Postgraduate School of Mechanical and Manufacturing Systems Engineering
Bradford University, Bradford, BD7 1DP, England

ABSTRACT

This paper contains a description of the principles of a flying hot-wire system, and outlines the advantages and disadvantages of using a hot-wire probe system based on either a circular, linear or 'bean shaped' curve path. The system developed at Bradford University is based on the 'bean shaped' curve path first utilized at Imperial College. A brief description is given of its operation. The validity of the system was demonstrated by a calibration test in which a single normal hot-wire probe was moved in still air. Finally, results are presented for measurements with such a probe behind a backward-facing step with a height H = 120 mm. The results obtained show many of the features observed in similar investigations with Laser-Doppler anemometry, but some new bi-modal phenomena are noticed in the pdf curves in parts of the separated flow region. It is demonstrated that this bi-modal phenomena is consistent with the existence of a flip-flop stability situation in the shear layer, which bounds the separated flow region.

1. INTRODUCTION

Hot-wire anemometry is a useful and practical tool for the study of many turbulent flows. A single normal hot-wire probe is easy to use and can provide information on the longitudinal velocity component in low/moderate turbulence intensity flows. However with a single stationary hot-wire probe one is not able to detect reversals in the flow direction. To measure the lateral velocity components a variety of probe configurations are commercially available with one, two or three wire sensors, the output from which can be manipulated to obtain the desired quantities. Tutu and Chevray [1] carried out an extensive study of the effects of large velocity fluctuations on the output of an X hot-wire probe including errors caused by flow reversals. In practice it has been found that to obtain reliable results the (U,V) velocity vector must lie within the approach quadrant of the X-probe.

For these reasons it has, until recently, proved difficult to obtain reliable quantitative experimental information on the velocity field in regions of separated flow. However, due to the development of more complex techniques such as the flying hot-wire technique, the pulsed hot-wire anemometer and Laser-Doppler anemometer, detailed flow measurements in separated flow regions are now possible. This paper is concerned with the flying hot-wire technique. Basically, a hot-wire probe responds to the velocity vector relative to a wire-fixed co-ordinate system. This principle is used in all flying hot-wire techniques. To avoid the signal rectification associated with stationary probes in reversing flows, the probe is moved through the region of interest with a known velocity, higher than any instantaneous negative velocity. Various implementations of this technique are considered in this paper, and the advantages and disadvantages, of systems utilizing a circular, a linear and a 'bean shaped' probe path are discussed. The 'bean shaped' path was selected in the flying hot-wire probe system developed at Bradford University, and this paper gives a brief description of its implementation. Initially the system was tested using a single normal hot-wire probe. A calibration test was first carried out in still air to demonstrate the accuracy of the system. This was followed by a test involving measurements behind a backward-facing step.

2. THE FLYING HOT-WIRE TECHNIQUE

The basic principle of the flying hot-wire technique can be explained with reference to figure 1. It is assumed that we have a surface with a separated flow region. A space-fixed co-ordinate system (X, Y) is introduced, in which the flow velocity vector $\vec{V}$ and the related velocity components (U, V) are to be evaluated. (In this discussion only a two dimensional flow field is considered.) For a given

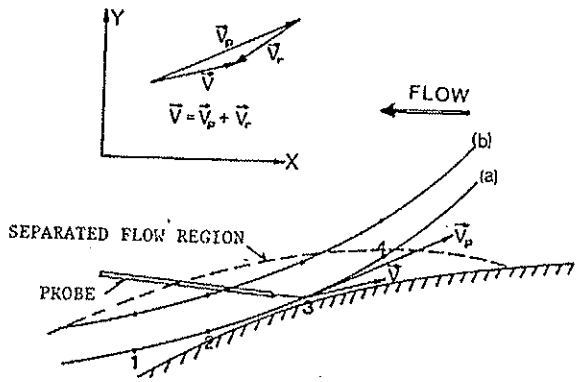

Fig 1 Principle of measurement with a flying hot-wire probe.

geometry the sensor of the flying hot-wire will follow a prescribed curve say (a). At some time t, the probe position (X_p, Y_p) will be at, eg location (3) and the probe will be moving with a velocity $\vec{V}_p$. Both the probe position and velocity are assumed to be known. The corresponding velocity of the flow is $\vec{V}$. The relative velocity $\vec{V}_r$ seen by the probe is obtained from the vector relationship

$$\vec{V} = \vec{V}_p + \vec{V}_r \qquad (1)$$

as illustrated in figure 1. If $|\vec{V}_p|$ is always greater than the instantaneous values of $|\vec{V}|$ then the direction of $\vec{V}_r$ will never "reverse", and the hot-wire signal can be interpreted uniquely. Thus during a sweep, at any prespecified point (say (3)) we can evaluate the related velocity $\vec{V}$, and the corresponding velocity components (U, V). This procedure can be repeated for a number of points along the curve path (a) during a single sweep. To obtain statistical quantities, such as the mean and rms values of the U and V velocity components at specified points, it is necessary to use ensemble averaging techniques. For this purpose the sweep must be repeated many times. When these sweeps are completed then the related data analysis will provide the required results for the selected points. To map the complete separated flow region it is necessary for the flying hot-wire system to be mounted on a traversing mechanism which permits the system to be moved both in the X and Y direction. By moving the system in, eg the Y direction, a similar curve (b) will be obtained intersecting a different part of the separated flow region. Repeating the procedure described for curve (a) will provide the required velocity quantities for selected points on curve (b). This procedure is repeated until the separated flow region has been fully covered.

2.1 Implementation of the Flying Hot-wire Technique

To demonstrate the implementation of a flying hot-wire system the following three different probe paths and related mechanisms are discussed:
1. A circular motion as used at the California Institute of Technology (CIT), (Cantwell [2], Wadcock [3] and Coles and Wadcock [4]. 2. A linear motion as used at Melbourne University (MU) (Watmuff et al [5], Perry [6]). 3. A curve linear 'bean shape' motion as used at Imperial College (IC) (Thompson [7], Thompson and Whitelaw [8] and Thompson [9]). This motion was adopted in the present investigation.

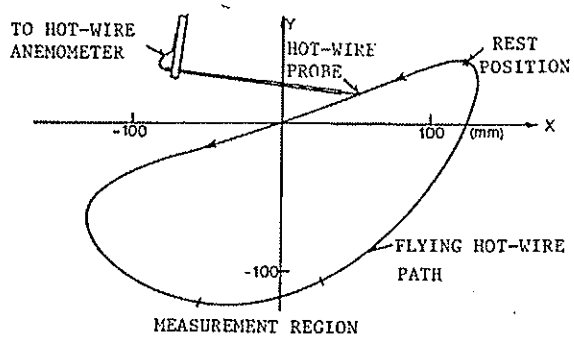

Fig 2 'Bean-shaped' curve pattern and related X, Y co-ordinate system.

Kinematics Having selected a curve path, the information required is the variation in the probe position (X_p, Y_p) and the corresponding probe velocity $\vec{V}_p$.

Mechanical Implementation Having chosen a probe path and a related variation in the probe velocity $\vec{V}_p$, a mechanical device has to be constructed, which can implement this motion. The circular motion used at CIT was obtained by placing the probe at the end of a (0.75 m) long, thin rotor arm. However, this configuration was prone to vibrations. The linear motion used at MU was achieved by placing the probe on a sled mounted on a rail. To reduce the friction between the sled and the rail, a special air bearing was mounted on the sled. The 'bean shaped' motion (see figure 2) used at IC and also in the current investigation was obtained using the four bar mechanism illustrated in figure 3. Mechanically, the motion is implemented by rotating a flywheel linked to the arm OR. This motion is obviously more complex than the circular motion used at CIT. However, in the CIT investigation the drive mechanism had to be placed inside the wind tunnel, thus creating a significant obstruction of the flow. For the four bar mechanism (figure 3) only part of the arm and the probe needs to be placed inside the wind tunnel, thus minimising the blockage effect.

Drive mechanism The circular motion used at CIT was maintained at a virtually constant angular velocity ω. Due to variation in the drag force during rotation, the motor driving the rotor arm had to be linked to a control system to maintain constant ω. An electric motor was also used to drive the flywheel of the four bar mechanism. However, in this system, the mechanism (and the probe) starts from rest (see figure 2) and significant angular accelerations are required in order to achieve the required magnitude of the probe velocity $\vec{V}_p$ during a single sweep. Consequently to avoid excessive torque requirements the mass of the rotat-

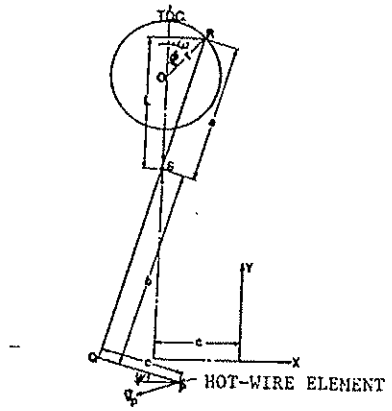

Fig 3 Principle of flying hot-wire probe drive mechanism. a = 0.16 m, b = 0.360 m, c = 0.130 m, r = 0.06 m.

ing parts of the system was minimized, and a DC printed circuit motor of a reasonably small size (≈ 1 kg) was selected. This type of motor could be overrun for a small period of time above its normal operating current, to achieve the high acceleration required during its first revolution. It could also be controlled easily for start/stop operations. The linear motion utilized at MU was operated on a continuous basis in the form of a linear pendulum motion. Consequently a complex mechanical system is required for the arresting, reversing and accelerating of the probe at either end of the motion. Also the linear motion of the probe may intersect the model under study, and to avoid impact the model must split open just before the probe reaches it.

Probe position and velocity In all three methods it is necessary to prespecify the positions at which measurements are to be carried out and to evaluate the corresponding probe velocity. In the case of a linear motion the probe velocity $\vec{V}_p$ usually set equal to $\{U_p, 0\}$ can under conditions of nearly constant velocity be evaluated from

$$U_p = \Delta X/\Delta t \qquad (2)$$

by measuring the time Δt corresponding to a specified distance ΔX. Similarly, for a circular motion the magnitude of the probe velocity $|\vec{V}_p|$ can be calculated from

$$|\vec{V}_p| = \omega r \qquad (3)$$

where r is the probe radius. Under conditions of nearly constant angular velocity, the value of ω can be obtained from

$$\omega = \Delta\phi/\Delta t \qquad (4)$$

by measuring the time Δt corresponding to a specified angle variation $\Delta\phi$. Based on the derivations given by Thompson and Whitelaw [8] and using the notation and co-ordinate system illustrated in figure 3, it can be shown that the probe position (X_p, Y_p) corresponding to the angle ϕ is given by

$$X_p = -r(b/a)\sin\phi + (c/a)L - c \qquad (5)$$

$$Y_p = a + b - r + r\cos\phi - (1+b/a)L - r(c/a)\sin\phi \qquad (6)$$

For convenience, the distance L, illustrated on figure 3 has been included in these equations,

$$L = (a^2 - (r\sin\phi)^2)^{\frac{1}{2}} \qquad (7)$$

The probe velocity components (U_p, V_p) in the (X, Y) co-ordinate system are obtained by differentiating equations 5 and 6 with respect to time (t) and setting $d\phi/dt = \omega$, giving

$$U_p = dx/dt = -\omega r\{\frac{b}{a}\cos\phi + \frac{cr\sin 2\phi}{2aL}\} \qquad (8)$$

$$V_p = dy/dt = \omega r\{(1+b/a)(\frac{r\sin 2\phi}{2L}) - \sin\phi - \frac{c}{a}\cos\phi\} \qquad (9)$$

These equations demonstrate that the instantaneous velocity of the probe can be determined provided ω and ϕ are known at that instant. As for the circular motion the value of ω can be obtained using eq 4. The angle ψ which the probe and its support makes with the X axis is required for measurements with an X hot-wire probe. From the geometry in figure 3, it can be shown that the angle ψ can be evaluated from

$$\psi = -\text{arc sin}\{r\sin\phi/a\} \qquad (10)$$

Equations 3 to 9 demonstrate that it is possible to determine the position and related probe velocity for both the circular motion and the four bar mechanism provided ϕ and ω are known. This information can be obtained by fixing a rotary encoder to the shaft of the driving motor. By monitoring the pulses from the encoder and hence the related angle ϕ, the position of the probe can be evaluated. Also by measuring the time interval between consecutive pulses the corresponding angular velocity ω can be evaluated from eq 4. A similar principle was applied at MU using a linear encoder system in the form of a grating system which created a Moire fringe pattern as a the sled moved past it.

Hot-wire probe calibration and signal interpretation All hot-wire probes, stationary or flying ones, are secondary devices, ie they need calibration before use. For a single normal hot-wire

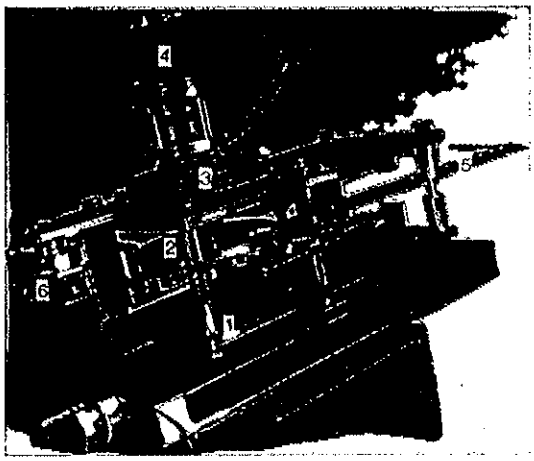

Fig 4 Photograph of flying hot-wire probe system

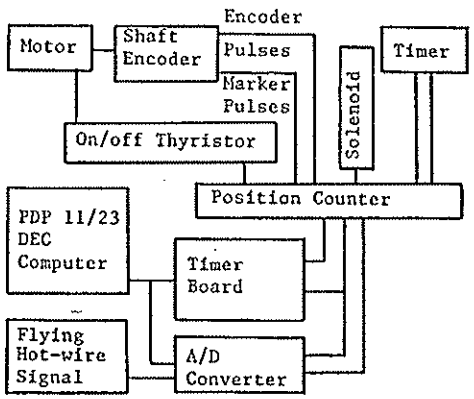

Fig 5 Flying hot-wire probe system block diagram

ing parts of the system was minimized, and a DC printed circuit motor of a reasonably small size (≈ 1 kg) was selected. This type of motor could be overrun for a small period of time above its normal operating current, to achieve the high acceleration required during its first revolution. It could also be controlled easily for start/stop operations. The linear motion utilized at MU was operated on a continuous basis in the form of a linear pendulum motion. Consequently a complex mechanical system is required for the arresting, reversing and accelerating of the probe at either end of the motion. Also the linear motion of the probe may interact the model under study, and to avoid impact the model must split open just before the probe reaches it.

Probe position and velocity In all three methods it is necessary to prespecify the positions at which measurements are to be carried out and to evaluate the corresponding probe velocity. In the case of a linear motion the probe velocity $\vec{V}_p$ usually set equal to $(U_p, 0)$ can under conditions of nearly constant velocity be evaluated from

$$U_p = \Delta X/\Delta t \qquad (2)$$

by measuring the time Δt corresponding to a specified distance ΔX. Similarly, for a circular motion the magnitude of the probe velocity $|\vec{V}_p|$ can be calculated from

$$|\vec{V}_p| = \omega r \qquad (3)$$

where r is the probe radius. Under conditions of nearly constant angular velocity, the value of ω can be obtained from

$$\omega = \Delta\phi/\Delta t \qquad (4)$$

by measuring the time Δt corresponding to a specified angle variation $\Delta\phi$. Based on the derivations given by Thompson and Whitelaw [8] and using the notation and co-ordinate system illustrated in figure 3, it can be shown that the probe position (X_p, Y_p) corresponding to the angle ϕ is given by

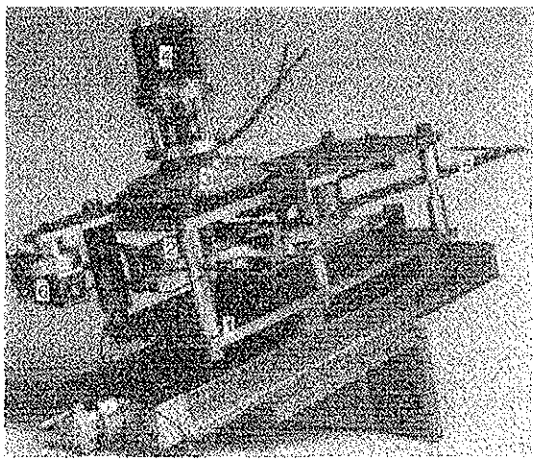

Fig 4 Photograph of flying hot-wire probe system

$$X_p = -r(b/a)\sin\phi + (c/a)L - c \qquad (5)$$

$$Y_p = a + b - r + r\cos\phi - (1+b/a)L - r(c/a)\sin\phi \qquad (6)$$

For convenience, the distance L, illustrated on figure 3 has been included in these equations,

$$L = (a^2 - (r\sin\phi)^2)^{\frac{1}{2}} \qquad (7)$$

The probe velocity components (U_p, V_p) in the (X, Y) co-ordinate system are obtained by differentiating equations 5 and 6 with respect to time (t) and setting $d\phi/dt = \omega$, giving

$$U_p = dx/dt = -\omega r\left(\frac{b}{a}\cos\phi + \frac{cr\sin 2\phi}{2aL}\right) \qquad (8)$$

$$V_p = dy/dt = \omega r\left((1+b/a)\left(\frac{r\sin 2\phi}{2L}\right) - \sin\phi - \frac{c}{a}\cos\phi\right) \qquad (9)$$

These equations demonstrate that the instantaneous velocity of the probe can be determined provided ω and ϕ are known at that instant. As for the circular motion the value of ω can be obtained using eq 4. The angle ψ which the probe and its support makes with the X axis is required for measurements with an X hot-wire probe. From the geometry in figure 3, it can be shown that the angle ψ can be evaluated from

$$\psi = -\text{arc sin}\,(r\sin\phi/a) \qquad (10)$$

Equations 3 to 9 demonstrate that it is possible to determine the position and related probe velocity for both the circular motion and the four bar mechanism provided ϕ and ω are known. This information can be obtained by fixing a rotary encoder to the shaft of the driving motor. By monitoring the pulses from the encoder and hence the related angle ϕ, the position of the probe can be evaluated. Also by measuring the time interval between consecutive pulses the corresponding angular velocity ω can be evaluated from eq 4. A similar principle was applied at MU using a linear encoder system in the form of a grating system which created a Moire fringe pattern as a the sled moved past it.

Hot-wire probe calibration and signal interpretation All hot-wire probes, stationary or flying ones, are secondary devices, ie they need calibration before use. For a single normal hot-wire

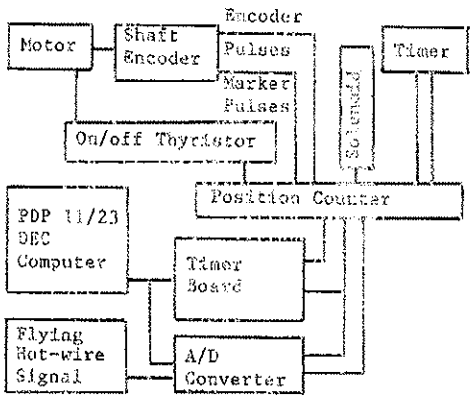

Fig 5 Flying hot-wire probe system block diagram

probe with the velocity V perpendicular to the sensing element, the relationship between E and V can, with a good degree of accuracy, be expressed in the form of a simple power law.

$$E^2 = A + BV^n \qquad (11)$$

The calibration procedure evaluates the calibration constants A, B and n (see Bruun et al [10]).

If the velocity vector $\vec{V}$ has both a U and V component, then an X hot-wire probe is often used. However, the signal interpretation of an X hot-wire probe will be discussed in a later paper, as this study only contains results for a single normal hot-wire probe.

Measurements with a flying hot-wire probe The pulses from the encoder were used to initiate data acquisition at specific probe positions. For all three types the data acquired consisted of a) the time Δt for one (or more) pulse period(s) and b) a single E value (normal probe) or double voltage values (E_1, E_2) from the two wires of an X hot-wire probe. This procedure was repeated for each of the specified acquisition positions. The time information Δt was, as explained previously, used to evaluate the probe velocity $\vec{V}_p$, and the anemometer signal(s) enabled the evaluation of the relative velocity $\vec{V}_r$. The corresponding flow velocity $\vec{V}$ was then obtained using eq 1.

3. OPERATION OF THE FLYING HOT-WIRE SYSTEM

The present flying hot-wire mechanism was based on the IC design. It was developed for the investigation of separated flows, such as the flow over the suction surface of an airfoil at high angle of attack, placed in a low speed open loop wind tunnel having a square working section of 61 cm x 61 cm. The maximum working section velocity was 25 m/s, and the maximum probe velocity used to date was 6 m/s. The flying hot-wire mechanism was mounted above the wind tunnel on a supporting frame, exterior to the wind tunnel.

Figure 4 shows the mechanical part and linked electrical components of the flying hot-wire system initially used at Bradford University with the key components identified as numbers 1-6. In addition, to the traversing mechanism (marked HTR 48) these components are: 1) a main assembly, consisting of two rectangular plates spaced 96 mm apart, onto which all other components are mounted. 2) A 140 mm nominal diameter and 8 mm thick flywheel, which is coupled to 3) a DC printed circuit motor. 4) A rotary encoder is also coupled to the shaft of the motor. 5) Attached to the perimeter of the flywheel is a 541 mm long flying arm with a probe mounted at the free end. Finally to arrest the motion of the probe after a single sweep the system also contains 6) a braking mechanism operated by a solenoid. The details of this system are described in Jaju [11].

The schematic diagram in figure 5 shows how the main electronic elements are related. To illustrate the overall operation of the system, the sequence of events for a single sweep is outlined below:

1. A manual push button switch (or a 10-second timer) sends a control signal to start the motor thyristor.
2. Motor and shaft encoder start rotating, and when the encoder passes through a marker point, the position counter is reset and pulses are counted from zero.
3. When the start of the measuring region is reached a DMA mode data acquisition is initiated. The start position is specified in the software as a selected value of the position counter reading. Data is transferred from the timing and hot-wire probe A/D boards to the computer's memory.
4. Transfer of data takes place each time an encoder pulse is encountered until the end of the measuring region, as specified in the software and the computer jumps to a waiting loop.
5. Motor switches off after a preset pulse count.
6. Motor continues rotation under inertia, and as it slows down, its speed is detected by a monostable circuit which activates a solenoid of a braking mechanism to arrest the flywheel.
7. Computer processes the data from this run, during the waiting time before another sweep.

TABLE 1

Calibration test for flying hot-wire probe system

A = 6.4454	B = 4.75320	n = 0.4277
Probe Velocity U_p (m/s)	Relative Velocity U_r (m/s)	$U_p - U_r$ (m/s)
5.764	5.742	0.022
5.759	5.700	0.059
5.778	5.652	0.126
5.758	5.647	0.111
5.771	5.667	0.104
$\langle U_p \rangle$ = 5.760	$\langle U_r \rangle$ = 5.680	

$$\frac{\langle U_p \rangle - \langle U_r \rangle}{\langle U_r \rangle} = 1.4\%$$

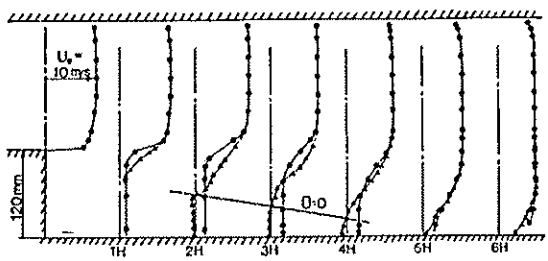

Fig 6 Mean velocity profiles measured with a flying hot-wire probe (▲) and a stationary hot-wire probe (●).

4. CALIBRATION

Tests were carried out using a single normal DISA 55P01 plated hot-wire probe operated at an overheat ratio of 1.8. This probe was initially calibrated statically using the DISA nozzle calibration facility. A typical set of calibration constants are shown in table 1. A flying hot-wire calibration test was then carried out in which the flying hot-wire probe was moved in still air, ie the flow velocity $\vec{V} = 0$. It therefore follows from eq 1 that

$$\vec{V}_r = -\vec{V}_p \qquad (12)$$

and the relative velocity $\vec{V}_r$ seen by the probe was thus equal in magnitude to the probe velocity $\vec{V}_p$. This relationship was used to test the flying hot-wire system by measuring $\vec{V}_r$ and $\vec{V}_p$ independently. The probe velocity $\vec{V}_p$ was evaluated at a single point by measuring the related time interval between two consecutive encoder pulses. Using eqs 5 and 6 a position $\phi \approx 159°$ was selected at which $\vec{V}_p$ was horizontal, but in principle any position on the probe path could have been used. Consequently in this test $\vec{V}_p = (U_p, 0)$. It therefore follows that $\vec{V}_r = (U_r, 0)$ and eq 12 can be written as

$$U_r = -U_p \qquad (13)$$

The related $\vec{V}_r = (U_r, 0)$ was evaluated from the hot-wire signal E in the form

$$E^2 = A + BU_r^n \qquad (14)$$

as U_r was perpendicular to the sensing element of the probe.

Typical values of U_r and U_p obtained from such a test are shown in table 1. The table contains the result of five individual sweeps and also the ensemble averages of 50 sweeps. As explained above the two velocities should theoretically be the same, and it is observed that the evaluated velocity U_r from the hot-wire signal is only about 1.4% lower than the encoder based velocity U_p. This discrepancy can partly be explained by a blockage correction effect in the nozzle calibration facility as reported by Khan et al [12].

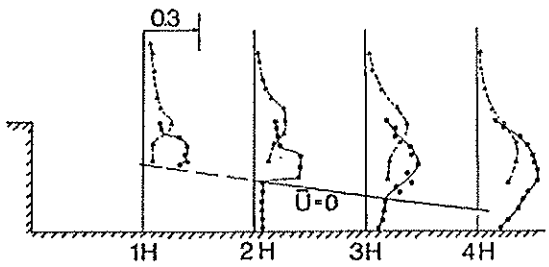

Fig 7 rms profiles (u'/U_o) measured with a flying hot-wire probe (●) and a stationary hot-wire probe (△).

5. BACKWARD FACING STEP

As stated earlier, the current test programme for the flying hot-wire system relates to separated flow on air foils. However, a short period was available prior to this investigation and during this period measurements were carried out in the separation region behind a backward-facing step. For these preliminary tests the system was operated with a single normal hot-wire probe. As for the calibration test described in section 4, data was acquired during a single sweep when $\phi \approx 159°$, ie when $\vec{V}_p = (U_p, 0)$. In the data analysis it was assumed that the measured relative velocity $\vec{V}_r = (U_r, 0)$. In a separated flow V_r is not zero, but the difference between $|\vec{V}_r|$ and U_r will in most part of the separated region be fairly small. The uncertainty caused by this assumption is discussed in the error analysis section. Using the above relationships for $\vec{V}_p$ and $\vec{V}_r$, the longitudinal velocity components of eq 1 can be expressed as

$$U = U_p + U_r \qquad (12)$$

Note from figure 1 that in this analysis U_r will have a negative value. Consequently the U velocity component of the flow vector $\vec{V}$ may have either a positive or negative value.

To study the flow behaviour in detail, a large backward-facing step, with a height H of 120 mm was selected. The test configuration is shown in figure 6. Upstream of the step a 0.8 m long plate spanned the width (0.61 m) of the wind tunnel. The distance from this plate to the top wall of the wind tunnel was 180 mm. The corresponding inlet velocity profile is shown in figure 6. The length of the plate downstream of the step was 10 H. Due to the initial mounting of the flying hot-wire system it was only possible to take measurements with the flying hot-wire probe inside the step height H, ie $0 < y \leq 120$ mm, and not in the free flow outside the separation region. However, this drawback was partly offset by traverses with a stationary normal hot-wire probe.

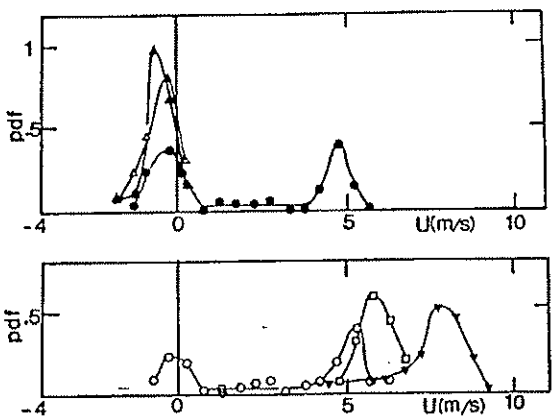

Fig 8 Probability density functions at X = 2 H evaluated from flying hot-wire probe data. Vertical positions: △:13 mm, ▲:43 mm, ●:63 mm, ○:83 mm, □:103 mm, ▼:120 mm.

Measurements with both a stationary and a flying hot-wire probe were carried out at axial locations 1H to 6H in steps of 1H. At each measurement point 100 sweeps were used for the flying hot-wire probe, whilst for the stationary hot-wire probe each sample record contained 2000 values taken over a period of 20 secs. The evaluated quantities were the mean ($\bar{U}$) and rms (u') values of the longitudinal velocity component and also selected pdf's. The measured mean velocity and rms profiles are shown in figure 6 and 7 respectively. The corresponding pdf's measured by the flying hot-wire probe system at X/H equal to 2 and 4 are shown in figures 8 and 9 respectively. As the stationary hot-wire results are unreliable in the separated flow region no pdf results are included for this probe type.

The results obtained confirm many of the features observed in previous experimental studies of backward-facing steps using either a Laser-Doppler anemometer (see eg Etheridge and Kemp [13], Tropea [14]) or a pulsed hot-wire anemometer (see eg Castro and Haque [15]). The results of eg Bradshaw and Wong [16] and Tropea [14] have demonstrated that the initial flow conditions and step geometry have a significant influence on the detailed developments in the separated flow region. The measured inlet velocity profile in figure 6 was found to be similar to the inlet conditions in the test case I investigated by Tropea [14]. Consequently a similar reattachment length $X_r/H = 4.5-5$ was found in both his and our investigations. The general shape and axial development of the mean velocity profiles shown in figure 6 were also similar to those reported by Tropea [14] and Etheridge and Kemp [13]. However, in our investigation the position of the curve corresponding to $\bar{U} = 0$ was found to occur at smaller values of y/H than in their investigations. This may be due to the use of a larger step height (120 mm) in our investigations as compared with Tropea (40 mm) and Etheridge and Kemp (13.5 mm). The corresponding rms profiles from both probes are shown in figure 7. In the region $X/H \approx 1-5$ the maximum value of u'/U_o in the investigation by Tropea (test case I) was about 0.13, as compared with a value of 0.23 in the study by Etheridge and Kemp. In the current investigation values of u'/U_o up to 0.32 were observed. These results appear to

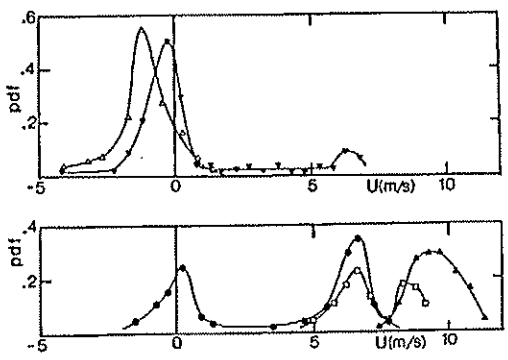

Fig 9 Probability density functions at X = 4H evaluated from flying hot-wire probe data. Vertical positions: △:13 mm, ▼:33 mm, ●:63 mm, □:103 mm, ▲:120 mm

indicate that both inlet condition and step geometry have a significant influence on the flow processes occurring inside the separated flow region.

The most distinct features were observed in the measured pdf's. As will be shown, the most likely reason for these significant differences from previous reported results is the use of a relatively large step height H of 120 mm, compared with those used in eg the investigations by Etheridge and Kemp [13] and Tropea [14]. The recent separated flow study by Castro and Haque [15] has demonstrated that a separated shear layer bounding a highly turbulent reverse-flow region has many features which are quite different from those of the plane mixing layer between two streams. The current results also demonstrate that the development in the shear layer bounding the separation region of a rearward-facing step will develop differently for small and large step heights. It was found that the variation in the pdf with y/H, as shown in figures 8 and 9, could be separated into three distinct regions. Firstly, for values of y/H below the curve $\bar{U} = 0$ a near normal distribution was observed with the peak centred around a negative mean velocity. The third region was observed near the outer edge of the shear layer (y/H ~1), where again a near normal distribution was observed centred around a positive mean value. The pdf curves obtained in these two regions are consistent with the Laser-Doppler anemometer results obtained by Tropea [14]. The pdf's measured by eg Tropea [14] showed a 'smooth' single peak transition from the near wall results to the free stream results outside the separated flow region. However, our measurements demonstrated a different phenomena on the 'inside' of the shear layer above the curve $\bar{U} = 0$. As can be seen from figure 7 this was the region with the highest values of u'. Both the results for X/H = 2 and 4 are similar, and the following discussion is presented in terms of the results at X/H ≈ 2 (figure 8). For all values of y below the $\bar{U} = 0$ curve (y ≈ 55 mm) similar single peaked pdf curves centred around a negative mean velocity of ≈ -0.5 m/s were observed. However, when the value of y was increased beyond the position of the $\bar{U} = 0$ curve, then a considerable change occurred in the pdf curves. The negative peak centred around -0.5 m/s was reduced in magnitude. In addition a positive tail of low probability was observed in the region 1-4 m/s followed by a second peak centred around U ≈ 4.5-5 m/s. This distinct pattern was observed at 5 different locations in the range y = 53-83 mm. As the probe was moved towards the outer part of the shear layer (y ≥ 93 mm) the negative peak disappeared and at y = 120 mm the signal again approached a normal distribution. This bimodal phenomena in the pdf curves can be explained in terms of the existence of a flip-flop situation for the shear layer bounding the separated flow region. In the case of a relatively large step height the shear layer is able to oscillate vertically over a considerable distance without a significant restraint being caused by the bottom wall. The pdf results indicate the existence of the following situation. The shear layer has two preferred (vertical) locations, referred to in the following as the upper and lower position with a rapid transition period between these two positions. This physical situation will result in the observed

bi-modal pdf's. When the shear layer is at its lowest position the probe will measure in the fast moving shear layer corresponding to the positive peak at U ≈ 5 m/s. When the shear layer is at the top position the reversed flow region will extend beyond the $\bar{U} = 0$ curve and the probe will record a negative value of U. As the change over from these two positions is very rapid, relatively few measurements will be obtained in this transitional region resulting in the very low probability observed in the velocity range 1-4 m/s. The nature of these results are compatible with the Laser-Doppler anemometer results obtained using smaller step heights. As the step height is reduced the bottom wall will start to restrict the vertical amplitude of the shear layer oscillations. This will result in the two peaks shown in figures 8 and 9 moving closer together until at some stage the two peaks merge into a single broad peak. This is of course the observation made by eg Tropea [14] using a step height of 40 mm.

In the outer part of the shear layer, differences were also observed between the results obtained with a stationary and a flying hot-wire probe as shown in figure 6 and 7. Originally it had been anticipated that there would have been a smooth transition from the flying hot-wire probe data to the stationary hot-wire probe data in this region. Moving beyond the separated flow region (X/H ≳ 5) such a smooth transition was observed (figure 6), but in the separated flow region itself considerable differences were noticed. Due to the single sweep principle of the flying hot-wire probe system and a rest period of 10 secs between each sweep it is likely that this probe will detect the naturally occurring separated flow. However, a stationary probe will modify the flow due to its continuous presence. This is usually of minor importance in low turbulence intensity flows, if a parallel support orientation is used, as it was in this test. However, the presence of the probe was found to have a significant influence on the unstable separated flow. As the probe was moved from the free stream flow into the shear layer, it was observed that the probe detected the existence of the free shear layer at a larger value of y than the flying hot-wire probe. This situation may be caused by the probe and its support influencing the normal flip-flop behaviour of the shear layer. As the stationary probe moves into the outer part of the shear layer it may cause the (local) shear layer to stay predominantly at its top position. This effect was observed in figure 7 as a vertical shift in the peak position of the u' distribution obtained with the stationary probe relative to the flying hot-wire probe results. The corresponding change in the mean velocity profiles is shown in figure 6. These results appear to indicate that even in the outer region of an unstable separated flow region, the results of a stationary hot-wire probe must be treated with great caution.

ERROR ANALYSIS

There were three main sources of errors in the evaluation of the flow velocity $\vec{V}$. The first is related to the accuracy of $\vec{V}_p$ and $\vec{V}_r$. From the calibration test it was estimated that both $\vec{V}_p$ and $\vec{V}_r$ were known to within ± 1-2% giving an uncertainty in $\vec{V}$ (eq 1) of about ± 2%. Secondly, the backward-facing step investigation was carried out with a single normal hot-wire probe, and the assumption that $V_r = 0$ introduced an additional uncertainty into the signal analysis. The magnitude of this error was estimated by considering the worst possible case in which the two components of the velocity vector $\vec{V}$ were of equal magnitude, ie $|U| = |V|$. From the related vector evaluation (eq 1) the error in the measured velocity component U_m was as follows: In the velocity range $U > 0$, the error increased nearly linearly with U with $(U_m - U)/U$ being about +12% at 2 m/s and +30% at 10 m/s. For negative velocities, the value of U_m/U was less than 1, with $(U_m - U)/U$ being about -10% at -1 m/s and -24% at -2 m/s. For values of $U < -3$ m/s non-unique values were obtained. In particular it should be noted that this error will not change the bi-modal nature of pdf curves, but only introduce a scaling error. This second type of error can of course be removed by the use of an X hot-wire probe. Finally, the number of samples N will affect the accuracy of the measured quantities. For the flying hot-wire probe system N = 100 and the time interval between each sample was 10 sec. Consequently the 100 samples were statistically independent. Furthermore when the measured probability density functions have a Gaussian distribution then specific procedures have been developed to describe the uncertainty related to the sample size (see eg Bendat and Piersol [17], and Bradbury and Castro [18]). However, in our case due to the bi-modal nature of several of the pdf's and the uncertainty introduced by the use of a single normal hot-wire probe, this error analysis aspect will be dealt with in further studies using an X hot-wire probe.

CONCLUSION

This paper has considered the flying hot-wire technique, outlining the main features of systems using a linear, circular or 'bean shaped' curve path. The implementation of the system at Bradford University has been discussed, and the accuracy demonstrated by a calibration test in still air. Results have been presented for measurements behind a backward-facing step. The measurements obtained with the flying hot-wire probe system are in agreement with many of the results quoted in previous studies. However, the pdf measurements demonstrated some unusual bi-modal features in some of the curves. It was concluded that this phenomena was due to the existence of a flip-flop stability situation in the shear layer that bounded the separated flow region.

ACKNOWLEDGEMENT

The authors wish to thank Professor J Whitelaw, Dr B E Thompson and the technical staff in the Mech Eng Dept at Imperial College for their advice in developing the flying hot-wire probe system at Bradford University. Also H'H Al-Kayiem wishes to acknowledge the scholarship awarded by the Mech Eng Dept, MTC, IRAQ, and M A Khan the award of a CASE-studentship by SERC and CEGB.

NOTATION

a	=	length (m)
b	=	length (m)
c	=	length (m)
E	=	probe signal (V)
(E_1, E_2)	=	probe signals from an X hot-wire probe
H	=	step height (m)
L	=	$(a^2 - (r\sin\phi)^2)^{\frac{1}{2}}$ (m)
$\vec{V}$	=	flow velocity vector (m/s)
$\lvert\vec{V}\rvert$	=	magnitude of flow velocity (m/s)
(U, V)	=	components of flow velocity (m/s)
$\vec{V}_p$	=	probe velocity vector (m/s)
(U_p, V_p)	=	components of probe velocity (m/s)
$\vec{V}_r$	=	relative flow velocity vector (m/s)
(U_r, V_r)	=	components of relative velocity (m/s)
$\langle U \rangle$	=	ensemble average of U (m/s)
$\bar{U}$	=	mean value of U (m/s)
u'	=	rms value of $u = U - \bar{U}$ (m/s)
U_o	=	inlet free stream velocity (m/s)
(X, Y)	=	space-fixed co-ordinate system (m)
(X_p, Y_p)	=	probe position (m)
ϕ	=	angle psoition (rad)
ω	=	angular velocity (rad/sec)

REFERENCES

1. Tutu, N K and Chevray, R, Cross wire anemometry in high intensity turbulence, J Fluid Mech, 71, 785-800, 1975.
2. Cantwell, B, A flying hot-wire study of the turbulent near wake of a circular cylinder at a Reynolds number of 140,000, PhD Thesis, California Institute of Technology, 1975.
3. Wadcock, A, A flying hot-wire study of two dimensional flow past an NACA 4412 airfoil at maximum lift, PhD Thesis, California Institute of Technology, 1977.
4. Coles, D and Wadcock, A J, Flying hot-wire study of flow past an NACA 4412 airfoil at maximum lift, J AIAA, 321-329, 1979.
5. Watmuff, J H, Perry, A E and Chong, M S, A flying hot-wire system, Experiment in fluids, 1, 63-71, 1983.
6. Perry, A E, Hot-wire Anemometry, Oxford: Clarendon Press, 1982.
7. Thompson, B E, Preliminary evaluation of flying hot-wire instrumentation, Imperial College, Mech Eng Dept, Report FS181/23, 1981.
8. Thompson, B E and Whitelaw, J H, Flying hot-wire anemometry, Experiments in fluids, 2, 47-55, 1984.
9. Thompson, B E, Appraisal of a flying hot-wire anemometer, Dantec Information, No 4, 14-18, 1987.
10. Bruun, H H, Khan, M A, Al-Kayiem, H H and Fardad, A A, Velocity calibration relationships for hot-wire anemometry, J Phys E : Sci Instr, 21, 225-232, 1988.
11. Jaju, A A R, Development of a flying hot-wire probe system, M Phil Thesis, Bradford University, 1987.
12. Khan, M K, MacKenzie, K A and Bruun, H H, Effects of blockage correction in hot-wire probe calibration facilities, J Phys E : Sci Instr, 20, 1031-1035, 1987.
13. Etheridge, D W and Kemp, P H, Measurement of turbulent flow downstream of a rearward-facing step, J Fluid Mech, 86, 545-566, 1978.
14. Tropea, C, Die turbulente stufenströmung in flachkanälen und offenen gerinnen, Doctor-Ingenieurs Dissertation, SFB80, Universität Karlsruhe, 1982.
15. Castro, I P and Haque, A, The structure of turbulent shear layer bounding a separation region, J Fluid Mech, 179, 439-468, 1987.
16. Bradshaw, P and Wong F Y F, The reattachment and relaxation of a turbulent shear layer, J Fluid Mech, 52, 113-135, 1972.
17. Bendat, J S and Piersol, A G, Random data : Analysis and measurement procedures, N Y, Wiley-Interscience, 1971.
18. Bradbury, L J S and Castro, I P, A pulsed-wire technique for velocity measurements in highly turbulent flows, J Fluid Mech, 49, 657-691, 1971.